ELSEVIER

## Contents lists available at ScienceDirect

# Hearing Research

journal homepage: www.elsevier.com/locate/heares



# Research Paper



# Investigation of intracochlear electrical fields with spread of excitation and voltage matrix in cochlear implant users and their link to speech perception

Pascal Nachtigäller<sup>a</sup>, Tobias Weissgerber<sup>b</sup>, Uwe Baumann<sup>b</sup>, Tobias Rader<sup>a,\*</sup>

- a Division of Audiology. Department of Otorhinolaryngology. LMU University Hospital. Ludwig-Maximilians-Universität München. 81377 Munich. Germany
- <sup>b</sup> Audiological Acoustics, Department of Otorhinolaryngology, University Hospital Frankfurt, Goethe University, 60590 Frankfurt am Main, Germany

#### ARTICLE INFO

# Keywords: Cochlear implant Spread of excitation Voltage matrix Transimpedance matrix ECAP Electric field

#### ABSTRACT

*Background:* Objective measures and their relation to listening performance are of interest in the study of cochlear implants (CIs). Both spread of excitation (SoE) and the voltage matrix (VM) are objective descriptors of electric field spread. VM is easier to measure and therefore preferable to SoE. The aim of the study was comparing both measurements postoperatively and investigating their relation to listening performance.

Methods: Postoperative SoE and VM data for 10 out of 17 CI-users were normalized to their maximum amplitude before comparison. A previously published SoE-width-based analysis method (Rader et al., 2023) was adapted and applied to the VM data. The ECAP separation index (from Hughes, 2008), comparing SoE data of two neighboring electrodes, was also adapted to the VM data of 17 CI-users and correlated with speech perception. Results: Recorded SoE and VM data correlated strongly in most CI-users. The normalized SoE and VM data showed good alignment. Some deviations were observable: an average RMS-difference of 0.159 normalized amplitude was found between SoE and VM data. Asymmetric width measures extracted from exponential fitting differed significantly between SoE and VM data. No correlation between width measures and speech perception could be found. The VM separation index correlated with speech perception.

Conclusions: SoE and VM are closely related measurements, however they are not identical. The neural information in SoE can't be ignored and VM can't replace SoE. The VM separation index appeared to be a promising approach for predicting listening performance. Nevertheless, further research is required to corroborate this finding.

# 1. Introduction

In cochlear implants (CIs), devices used to treat severe to profound hearing loss, an objective evaluation of the listening performance reached by the patient still proves difficult. The varying success between patients (Fetterman and Domico, 2002; Häußler et al., 2019; Rader et al., 2013) as well as the difficulty in judging whether the full potential has been exhausted, creates a desire for objective predictors of the listening performance possible for each CI-user. Several predictors and models have been explored already, but a consensus on them could not be formed yet.

In a previous study by the authors (Rader et al., 2023), the spread of excitation (SoE) was investigated as a possible predictor of the listening performance. SoE is an electrophysiological measurement, where the masking level of adjacent electrodes is derived through masked response measurements of the electrically evoked compound action potential

(ECAP), which is described in more detail in the previous study as well as in Abbas et al. (1999), Cohen et al. (2003), Miller et al. (2008). However, the measurement of SoE has some inherent limitations. For good response measurements, a high stimulation charge needs to be applied by the implant, ideally as high as the user tolerates at the least acceptable loudness level (LAPL). Since the stimulation charge is positively correlated to the quality of the recording (Rader et al., 2023), a higher charge is better and this might not be comfortable for the CI-user. Furthermore, the ECAP masking threshold needs to be measured for every electrode, leading to measurement times of around 7 min. Additionally, even if the SoE can be measured successfully, it can't always be interpreted. This is also described in more detail in the previous study Rader et al. (2023), where the measured SoEs were categorized according to their quality.

In this work, a different measurement is investigated alongside: the voltage matrix (VM, manufacturer MED-EL, Innsbruck, Austria). The

E-mail address: tobias.rader@med.uni-muenchen.de (T. Rader).

<sup>\*</sup> Corresponding author.

P. Nachtigäller et al. Hearing Research 465 (2025) 109357

voltage matrix is recorded by stimulating at one electrode and then measuring the voltage at another electrode. This is repeated for every combination of stimulating electrode and recording electrode, resulting in a matrix of voltages. The VM is measured through the impedance field telemetry (IFT), which also outputs the impedances and is routinely performed at the start of a fitting session. A related measurement is the transimpedance matrix (TIM, manufacturer Cochlear, Sydney, Australia), which also measures the voltages along the electrode array and divides them by the stimulation current, resulting in a matrix of impedances. Previous research on the VM mainly focused on monitoring the position of the electrode lead in the cochlea. The main application of the VM in monitoring the position of the electrode lead is the intraoperative detection of tip fold-overs. In the past, this was mainly done using the SoE-measurement (Grolman et al., 2009; Zuniga et al., 2017), but in recent years the focus has shifted towards the VM (Beck et al., 2024; Hans et al., 2021; Klabbers et al., 2021). A measurement of the insertion depth has also been shown to be possible through the VM (Aebischer et al., 2021), however the accuracy is not yet comparable to imaging methods like X-Rays or computed tomography (CT). An emerging field is the study of VM patterns for different etiologies (Vozzi et al., 2022; Wagner et al., 2020). They introduced the importance of acknowledging that there is a significant degree of variability in the VM results between CI users. Nevertheless, the observed range was found to be diminished when only users with a particular etiology are taken into consideration. Wagner et al. (2020) found more homogeneity in patients with intracochlear tumors with smaller current spread compared to their control group of average CI-users with the same implants but no stated homogeneity in their etiology. Vozzi et al. (2022) also found differences in the VM profiles among groups of CI-users with otosclerosis and congenital hearing loss.

Not much research has been dedicated to find a possible link between speech perception and metrics computed from the VM. Joly et al. (2021) introduced the electrical spread coefficient (ESC), which is calculated by rearranging the VM data and fitting the result with an exponential function. The ESC was found to correlate with the speech reception threshold (SRT) for disyllabic words in French, if the data for CI-users with deactivated electrodes was omitted. However, a more recent study by Wagner et al. (2023) found no effect of voltage gradients on monosyllabic word recognition. Kopsch et al. (2024) also investigated the influence of the TIM on monosyllabic word recognition and reported no correlation between TIM half-widths and speech recognition. For intraoperative measurements, Söderqvist et al. (2021) reported that SoE and normalized VM data correlate for most CI-users. Furthermore, the peak widths for SoE and VM data exhibited a high degree of alignment, indicating that both measurements overlap considerably. A very recent work by Mohan et al. (2024) also explored the relationship between SoE and TIM width data. They confirmed the findings of (Joly et al., 2021) and found weak correlations between the ESC and speech perception. They also investigated the relationship between width measures extracted from SoE and TIM, finding that there were differences in those metrics when grouped by age or gender. Additionally, they found no relation between speech perception and width measures extracted from SoE or TIM. A link between postoperatively recorded SoE and the TIM was investigated by Kopsch et al. (2022). For medial recording locations (electrode 13), they found a significant positive correlation between SoE and TIM half-widths, while apical and basal recording locations showed no correlation for SoE and TIM half-widths. A further investigation of the relation between SoE and VM data is one goal of the work presented in this work. Following up on the previous publication by Rader et al. (2023), this relationship is investigated postoperatively. Also of primary concern is an extension of the previously established evaluation method to the VM data and whether the results found for SoE can be reproduced with the VM data, especially the width measures and the correlation with SRT data. This is of particular interest, since the VM has some advantages to SoE, especially considering the quality and amount of the acquired data. Each measurement of the VM contains a voltage curve for

each electrode, which allows the implementation of different analysis approaches suggested in previous publications. Particularly the ECAP separation index introduced by Hughes (2008) is of interest here. This metric describes the spread of the electric field through the difference of two SoE measurements and was found to correlate with pitch ranking scores, which in turn is related to speech perception. Therefore, an adaptation of the ECAP separation index to the VM data and its relation to speech perception was investigated.

Summarily, this paper sets out three main aims. Firstly, the relation between SoE and VM data is considered postoperatively. Secondly, the previously established SoE analytical method is applied to VM data. Finally, further analysis methods from the literature are adapted for the dataset in question.

# 2. Methods

# 2.1. Participants and data acquisition

A total of 17 bilaterally implanted CI-users agreed to participate in this study. The participants are identical to the ones in the previous study by Rader et al. (2023): the age at the time of the experiment ranged from 14.6 to 77.9 years with an average age of 41.6 years and CI experience ranged from 1.6 to 15.4 years with an average of 9.0 years. The CI-users had either Combi 40+ (4), CONCERTO (17), PULSARci100 (8) or SONATAti100 (5) implants with Standard (10), Medium (1), Compressed (1), FlexSoft (7), Flex28 (10) and Flex24 (1) electrode arrays. This data along with the etiologies is also shown in Table 1. Of the 17 CI-users, 13 had at least one electrode deactivated in one of their CIs. CI-users are denoted in this paper with a number and the side of the ear, e.g., S11 refers to CI-user number 1, left ear and S1r refers to CI-user number 1, right ear.

The SoE recordings are likewise taken from this previous study. They were recorded using a spatial forward-masking paradigm (Abbas et al., 1999) with two stimuli, a masker and a probe presented in short order. The probe stimulus was spatially fixed and the masker varied across the electrode array. The resulting masked ECAP response to the probe stimulus was taken for each pair of probe and masker electrodes. The stimuli used were biphasic pulses with a pulse duration of 30  $\mu s$  and an interphase gap of 2.1  $\mu s$ , presented at LAPL. The delay between masker and probe stimuli was 400  $\mu s$ . Artefact reduction was achieved using the alternating polarity paradigm (Klop et al., 2004). SoE measurements were taken at three recording locations: apical (probe electrode 3), medial (probe electrode 6) and basal (probe electrode 9). The recoding electrode was the basally adjacent electrode of the probe electrode (4, 7 and 10 respectively).

The VM measurements were performed using the Impedance Field Telemetry (IFT) of the fitting software MAESTRO (MED-EL, Innsbruck, Austria). A biphasic pulse with a pulse duration of 24.17  $\mu s$ , an interphase gap of 2.1  $\mu s$  and an amplitude of 302.4 current units (cu, 1 cu  $\approx 1$   $\mu A$ ) is presented at a stimulating electrode and the resulting voltage is measured at all electrodes. From this, a 12  $\times$  12 matrix is constructed, containing the voltage drops between electrodes. For the remainder of this paper the stimulating electrode is also referred to as probe electrode, since it is analogous to the probe electrode in the SoE measurement. The VM was extracted from the participants' fitting-software exports using the scientific export function, giving an XML-file from which the VM can be extracted. Distances along the electrode array like contact spacing and electrode lengths were extrapolated using the schematic draw of the electrode arrays supplied by the manufacturer MED-EL.

The speech recognition threshold (SRT) data in this paper was measured using a matrix sentence test (Oldenburg sentence test, OLSA) in a multi-source noise field, utilizing the two noise conditions Fastlnoise (FN, modulated noise) and OL-noise (OL, unmodulated noise). The listening test setup used four loudspeakers located at the corners of a listening booth (azimuth  $\pm$  27° and  $\pm$  153°; distance to head center d= 169 cm; elevation above head 100 cm) to generate a diffuse noise field

and a speaker at  $0^{\circ}$  azimuth, 130 cm distance to deliver the target speech stimulus. More information on the OLSA and the noise conditions used can be found in Rader et al. (2013). This data was also identical to the data used in the previous study and a more detailed description on the SRT data collection can be found there.

#### 2.2. Normalization

To get the closest similarity between SoE and VM data, both measurements were normalized. Each SoE recording was normalized to a normalized amplitude of 0 for the minimum value and a normalized amplitude of 1 for the maximum value. For the VM, the diagonal elements corresponding to the near-field components of each voltage curve, were removed to get only the far-field components, since a relationship between VM and SoE was expected to lie in the far-field. Then the voltage curve corresponding to the SoE recording was extracted (e.g., for SoE with probe-electrode 3, the voltage curve of electrode 3 was taken). Those voltage curves had an inverse shape of the SoE recordings, so the voltage curves were inverted to fit the shape of the SoE recordings. Each voltage curve was then normalized to the second smallest value of the corresponding SoE recording for the minimum value and 1 for the maximum value. This was done because the diagonal element, which would be the smallest element, was removed. Finally, the previously removed diagonal element, analogous to the probe electrode value of the SoE recording, was set to 0 to get the closest match between SoE and VM data. A graphic representation of this normalization is shown in Fig. 1A. This normalization was done for each pair of SoE recording and voltage curve separately and referred to as min2-normalization in this

Alongside, another normalization approach was used in this paper, shown in Fig.1B. Here, first the diagonal elements were removed from the VM, followed by a division by its largest value such that the maximum value is equal to 1. This approach is referred to as whole-VM-normalization in this paper and used for the calculation of the VM separation index.

# 2.3. Data analysis

The SoE- and VM-data, normalized using the min2-normalization, were split into two halves along the probe electrode and each half fitted using an exponential function. From those fits, the measures of width and asymmetry were extracted using the same approach as outlined in our previous work (Rader et al., 2023). Accordingly, the extracted measures are the distances to 25 % and 50 % of the amplitude on the apical side, denoted as DIST $_{\rm a,0.25}$  and DIST $_{\rm a,0.5}$  respectively. The

same measures were also taken on the basal side, denoted  $DIST_{b,0.25}$  and  $DIST_{b,0.5}$ . Also, the sum of those distances was evaluated with  $DIST_{ab,0.25}$  =  $DIST_{a,0.25}$  +  $DIST_{b,0.25}$  and  $DIST_{ab,0.5}$  =  $DIST_{a,0.5}$  +  $DIST_{b,0.5}$ . The measure of asymmetry  $\Delta Max_{ab}$ , which is the difference in maximum amplitude on both sides, was extracted as well. Those measures are shown graphically in Fig. 2. The deviation between SoE and VM data was evaluated using the absolute difference curve between normalized SoE and VM data as well as the RMS of this difference curve.

As mentioned in the introduction, the ECAP separation index (Hughes, 2008) was adapted to the VM data, in the following referred to as VM separation index. For this, the VMs were first normalized using the whole-VM-normalization, from which two voltage curves were extracted. Those two curves were then used to calculate the VM separation index using the same formula stated in Hughes (2008):  $\sum_{i=1}^{22} |a_{xi} - a_{yi}|$ , where  $a_{xi}$  and  $a_{yi}$  are the ECAP amplitudes of the two SoE

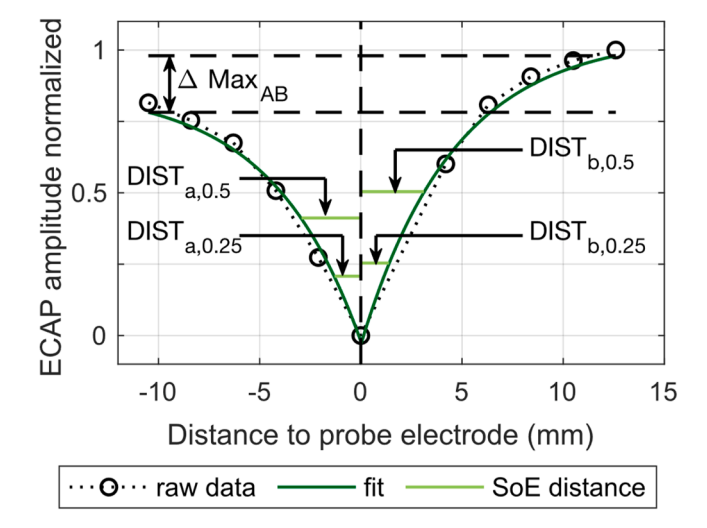


**Fig. 2.** Explanation of the different SoE measures extracted from the exponential fit. Dotted lines: connections of the actual individual recordings at adjacent electrodes. Solid lines (green): exponential fit, performed for the apical and basal side of the SoE recording separately. All measures are extracted from the exponential fits. DIST<sub>a,0.25</sub> and DIST<sub>a,0.5</sub> are the distances in mm from the probe electrode to 25 % and 50 % peak amplitude on the apical side respectively. Analogous, DIST<sub>b,0.25</sub> and DIST<sub>b,0.5</sub> are the distances to 25 % and 50 % peak amplitude on the basal side.  $\Delta$ Max<sub>ab</sub> is the difference in peak amplitude on the basal and apical sides, i.e., the measure of asymmetry between the apical and basal sides.

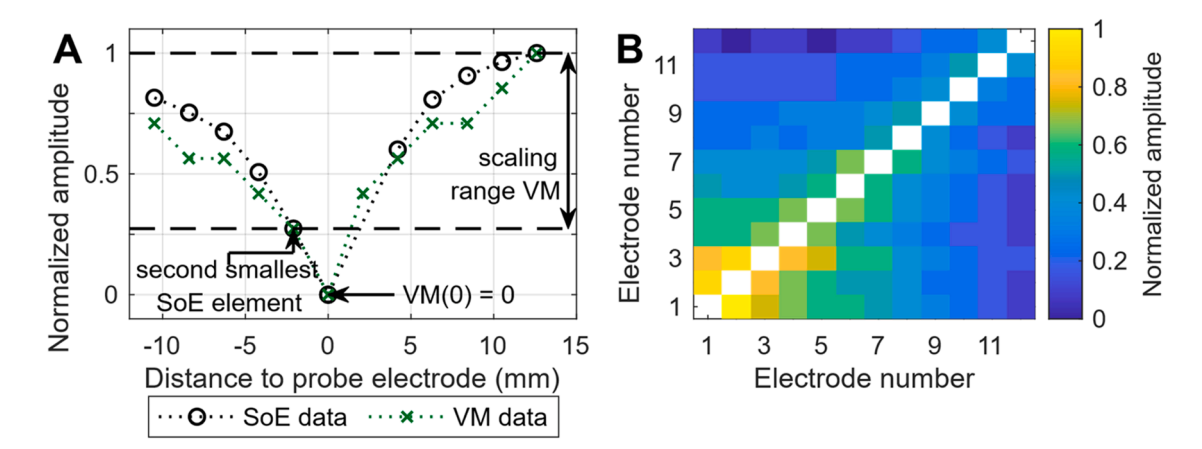


**Fig. 1.** Graphic representation of the normalization methods used. A: normalization of SoE and voltage curves from the VM, using the min2-normalization. SoE is normalized to the maximum value of 1 and the minimum value of 0. The VM is normalized such that the second smallest element has the same value as the second smallest SoE-element and the maximum is 1. Then, VM-element corresponding to the probe electrode is set to 0. B: normalization of the whole VM without the diagonal, denoted as whole-VM-normalization. Here, the entire VM is normalized by division through the largest element.

measurements  $a_x$  and  $a_y$  at each masker electrode i. The ECAP separation index was introduced for implants of the manufacturer Cochlear, which have 22 electrodes. For the MED-EL implants used in this work, this sum was adapted to  $\sum_{i=1}^{12} |a_{xi} - a_{yi}|$ , according to the number of electrodes in MED-EL implants. Here,  $a_{xi}$  and  $a_{yi}$  represent the normalized amplitudes of the voltage curves for two stimulating electrodes x and y at each recording electrode i. The calculation of the VM separation index is illustrated in Fig. 3. Similar to the analysis of the SoE, electrodes in the apical, medial and basal region were chosen as the baseline electrodes. Here, electrode 4 was chosen for the apical region, electrode 7 for the medial region and electrode 9 for the basal region. The neighboring electrodes used for the calculation of the VM separation index were  $\pm 1$  and  $\pm 2$  for the apical and basal regions and  $\pm 1$ ,  $\pm 2$  and  $\pm 3$  for the medial region.

#### 2.4. Statistical analysis

As all data collected in this paper was non-normal, nonparametric statistical testing was performed with a significance level of p = .05, using the software MATLAB (The MathWorks Inc, 2024). For correlation analysis, Spearman's correlation coefficient was calculated. The correlation between SoE and VM data was performed without the probe electrode. Significant differences between metrics were investigated using the Wilcoxon signed-rank test. Analogous to the previous paper, the data that was correlated with the bilaterally measured SRTs had to be processed additionally because the speech perception was measured in the bilaterally best aided condition. This was done in the same way as described in Rader et al. (2023). Two approaches were introduced there: the average approach, taking the average of the extracted parameters and the minimum approach, taking the minimum of both extracted parameters. I.e.,  $DIST_{a,0.25,mean} = \frac{1}{2} \left( DIST_{a,0.25,right} + DIST_{a,0.25,left} \right)$  and  $DIST_{a,0.25,min} = min((DIST_{a,0.25,right} + DIST_{a,0.25,left}))$ . For the correlation between VM separation index and SRTs, another processing method was evaluated: along with the average and minimum value of both ears the maximum value of the VM separation index of both ears was also considered because it was unclear whether the "better ear" would correspond to the minimum or the maximum of the VM separation index.

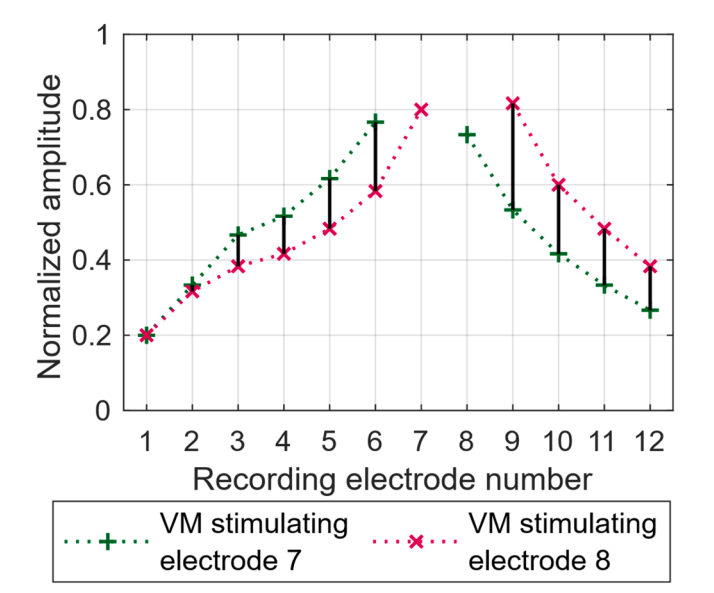


**Fig. 3.** Graphical representation of the VM separation index. The dark green curve is the voltage curves of stimulating electrode 7, the pink curve is the voltage curve of stimulating electrode 8, both extracted from the VM data and normalized using the whole-VM-normalization. The solid black lines are the differences between both voltage curves at the specified electrodes.

#### 3. Results

## 3.1. Comparison of SoE and VM data

SoE data at the apical recording location ranged from  $-124~\mu V$  to 1117 µV with a mean of 232.2 µV. For the medial recording location the data ranged from  $-43~\mu V$  to  $945~\mu V$  with a mean of  $207.2~\mu V$ . At the basal recording location, SoE data ranged from -78 µV to 1293 µV with a mean of 245.7  $\mu$ V. VM data without the diagonal entries fell between 3.8 mV and 608.7 mV with a mean of 134.1 mV. The comparison between SoE and VM data was limited by the number of analyzable curves collected in the previous study (Rader et al., 2023). There, only the data from 10 ears (7 CI-users) could be evaluated at all recording locations, giving analyzable data at the apical, medial and basal recording location. Accordingly, a comparison between SoE and VM could only be done for those 10 ears. Those are shown in Fig. 4, where a good match between the normalized SoE and VM data is visible. This similarity can also be seen in the correlations between both measurements. For most cases, SoE and VM data were highly correlated. At the apical recording location (probe electrode 3) all correlations were significant with high correlation coefficients r of 0.77 to 0.99. At the medial recording location (probe electrode 6), two ears did not show a significant correlation: both ears of S16 (S16l p = .062 and S16r p = .072). In the remaining ears however, SoE and VM data were highly correlated with coefficients between 0.85 and 0.96. The basal recording location (probe electrode 9) showed the least number of significant correlations. Here, four ears had uncorrelated SoE and VM data: S1r, S11l, S16r and S16l. The correlation coefficients and their significances are shown in more detail in Fig. 4.

Apart from the correlation, the similarity was also investigated using the difference between SoE and VM data. This is shown in Fig. 5, where the absolute difference between both curves is plotted. A couple of observations can be made here. First, it is quite visible which points are used for the normalization, as in general the difference at those points (the maximum value and the value of the probe electrode) is 0. Only at the apical recording locations were two ears which differed: S16r and S16l had their SoE minimum amplitude not at the probe electrode but shifted one electrode to the apex. This results in larger curve differences for those two ears. Another observation was, that the greatest differences between the curves mostly appeared one or two electrodes in the basal direction from the probe electrode, indicating that the slope towards the basal direction is shallower for the voltage curves. The difference between SoE and VM data was quite varied between the different ears and recording locations. This was also reflected in the RMS-differences, which ranged from 0.046 to 0.27 normalized amplitude for the apical recording location, 0.1 to 0.27 for the medial recording location and 0.074 to 0.24 for the basal recording location. The detailed numbers of the RMS-differences are shown in Fig. 5 and a boxplot of the RMS-differences is shown in Fig. 6 grouped by recording locations as well as the average across all recording locations. This average showed a smaller spread than the recording locations by themselves, the range there was reduced to 0.093 to 0.22.

# 3.2. Evaluating the VM using SoE-fitting

The exponential fitting and parameter extraction as described in Section 2.3 and Fig. 2 could also be performed on the normalized voltage curves extracted from the VM. Like in the previous paragraph, here again some differences between SoE and VM data could be found. Boxplots of the extracted parameters are shown in Fig. 7A, together with the SoE-data from the previous study. For the apical recording location (Fig. 7A, top), the extracted parameters are very similar with the VM data showing slightly smaller spread than the SoE data. However, for the summed distances DIST<sub>ab,0.25</sub> and DIST<sub>ab,0.5</sub>, the difference between SoE and VM data was found to be significant (Wilcoxon signed-rank test p = .0039 and p = .027 respectively). The medial recording location (Fig. 7A, middle) also showed significant differences in extracted

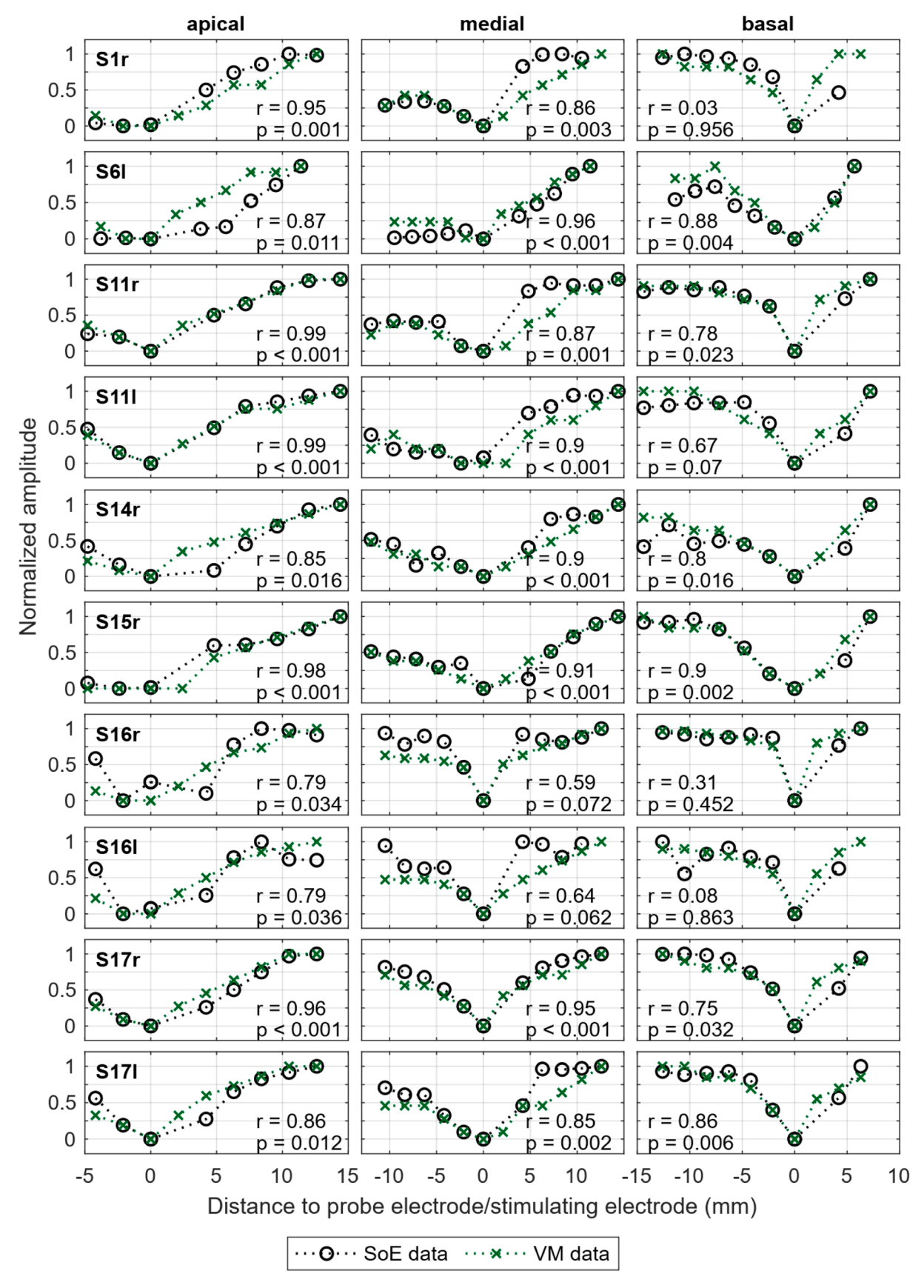


Fig. 4. Normalized ECAP (dotted black lines with circles) and voltage amplitudes (dotted green lines with crosses) of the SoE and VM measurements, normalized using the min2-normalization. The recording locations apical, medial and basal used the probe/stimulating electrodes 3, 6 and 9 respectively. Alongside, the correlation coefficient r and significance p are shown. Distances were extrapolated using a schematic draw of the electrode array provided by the manufacturer.

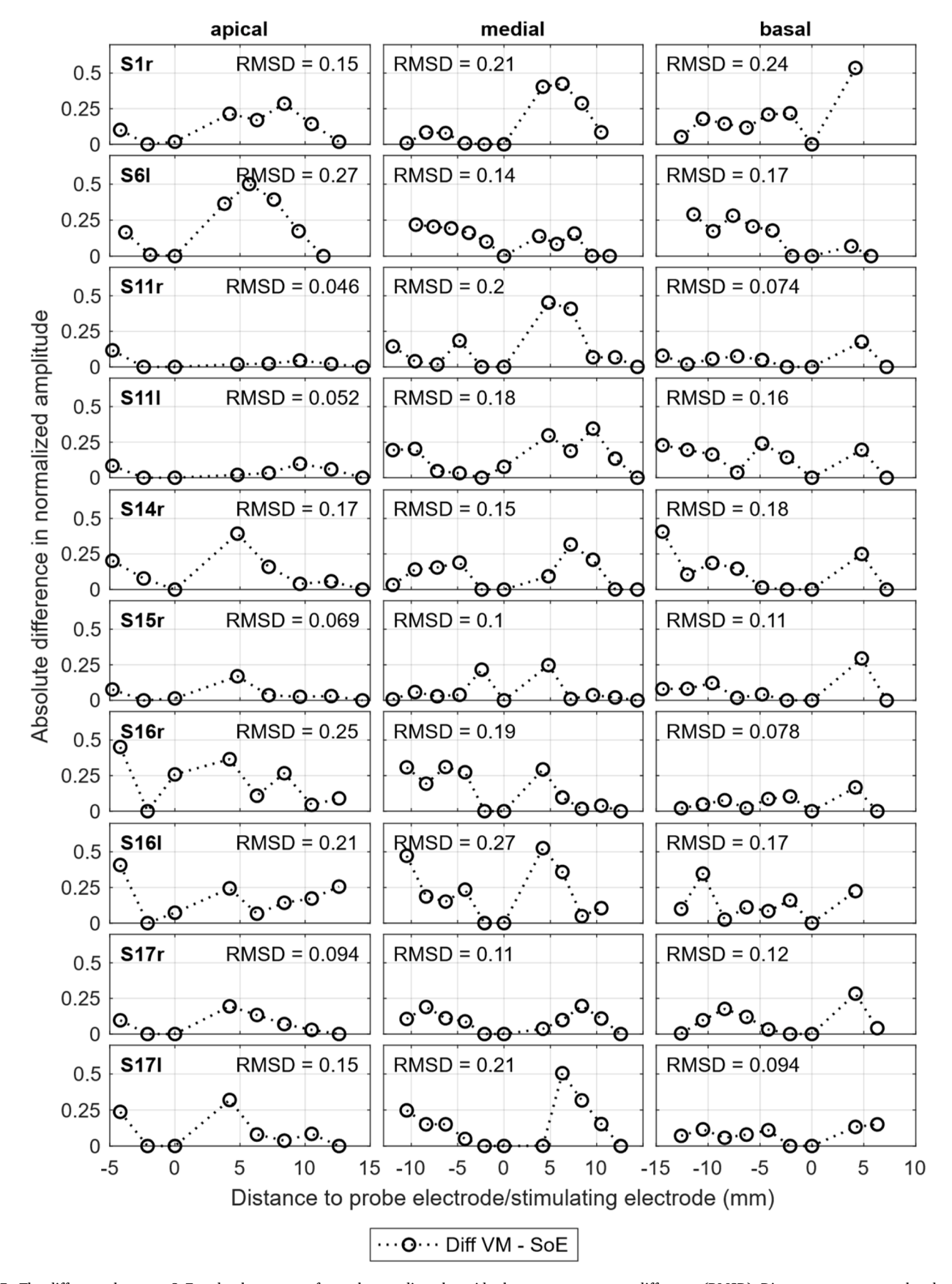
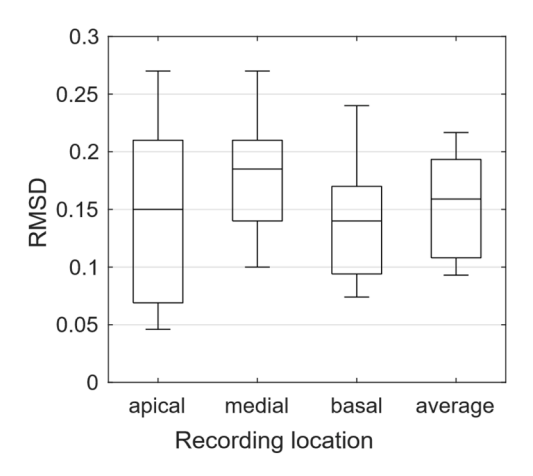


Fig. 5. The difference between SoE and voltage curve for each recording alongside the root mean square difference (RMSD). Distances were extrapolated using a schematic draw of the electrode array provided by the manufacturer.



**Fig. 6.** Boxplots of the root mean square difference (RMSD) for each recording location and the average across all recording locations.

parameters, here  ${\rm DIST_{b,0.25}}$ ,  ${\rm DIST_{b,0.5}}$  and  ${\rm DIST_{ab,0.5}}$  deviated between SoE and VM data (Wilcoxon signed-rank test p=.049, p=.037 and p=.002 respectively). A larger spread for the VM-extracted parameters is also visible in the boxplots. The largest differences between SoE and VM data occurred at the basal recording location (Fig. 7A, bottom). Four parameters were found to differ significantly:  ${\rm DIST_{a,0.25}}$  (p=.002),  ${\rm DIST_{b,0.25}}$  (p=.014),  ${\rm DIST_{a,0.5}}$  (p=.002) and  ${\rm DIST_{b,0.5}}$  (p=.014). The measure of asymmetry  ${\rm \Delta Max_{ab}}$  (Fig. 7B) did not show significant differences between SoE and VM data for any of the three recording locations. The correlation with SRTs performed in the previous study was repeated for the parameters extracted from the VM data, however the significant correlations present with the SoE-parameters could not be reproduced.

# 3.3. VM separation index

In order to achieve increased accuracy in the calculation of the VM separation index, the following section incorporates data from a greater number of subjects. Here, the VM could be obtained for every ear of every CI-user (n = 17) for a total of 34 VMs. The results of the VM separation index with the chosen electrodes are shown in Fig. 8. Unsurprisingly, with increasing spacing between the electrodes, the VM separation index increased alongside. Interestingly however, the asymmetry seen in maximum ECAP amplitude of both halves of the SoE measurement discussed in the previous study (Rader et al., 2023) was also present in the VM separation index, where an asymmetry between the more apical and more basal comparison electrodes is visible. This effect was not apparent for the VM separation index between two adjacent electrodes, but for larger spacings like two or three electrodes distance, a greater VM separation index for the comparison with a more basal electrode could be observed. For the apical electrode 4, no significant difference was found between the VM separation index towards the base and the VM separation index towards the apex. However, Fig. 8 depicts a higher value for the more basal VM separation index. The VM separation index between electrodes 7-4 and 7-10 were found to be significantly different (Wilcoxon sign-rank test p < .001) as well as the VM separation index between electrodes 9-7 and 9-11 (Wilcoxon sign-rank test p = .036).

The VM separation index was also correlated with the SRTs obtained in the previous study. For 2 subjects (S4 and S8), no SRT data could be obtained, therefore they were excluded from this correlation analysis. As mentioned in the previous section, the VM separation index was calculated for each ear separately, but for the correlation the data from both ears had to be combined into one value. For this, three options were investigated: the minimum, the mean and the maximum VM separation index of both ears. The VM separation index varied between both ears

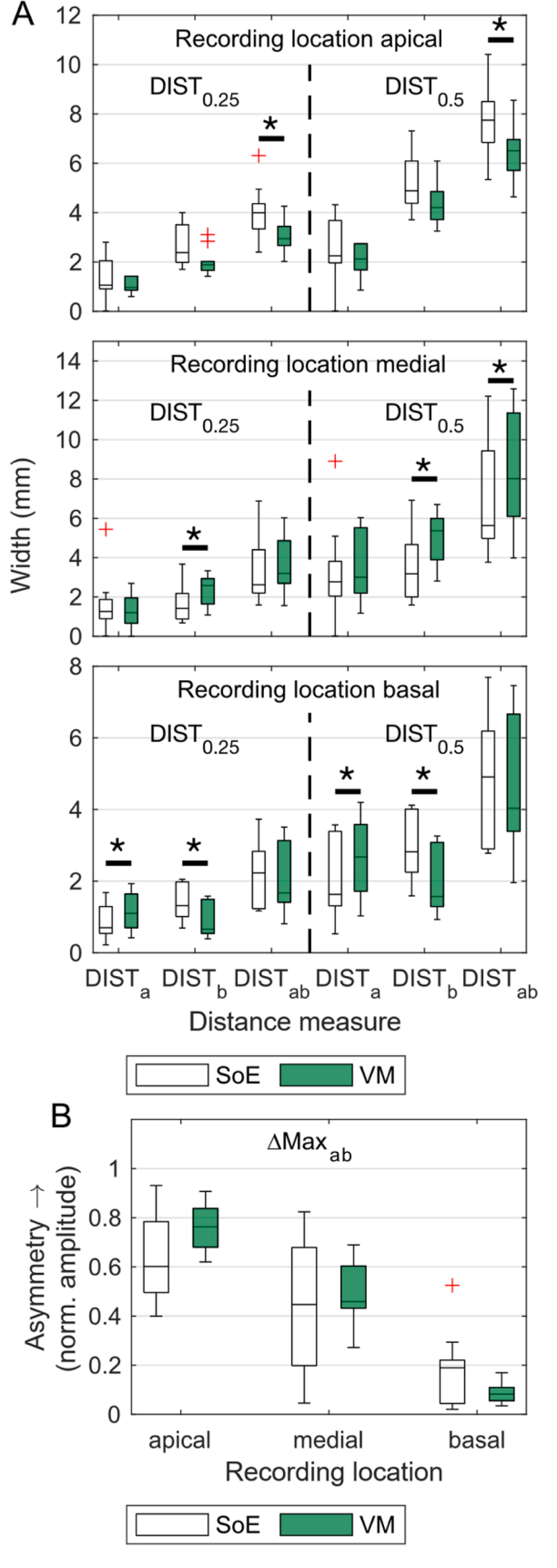
with a maximum difference between ears of 2.57, a mean difference between ears of 0.019 and an interquartile range of 0.92. For the mean of both ears, significant correlations were found between the VM separation index of electrodes 7–8 and the FN-SRTs (p < .001, r = -0.8) as well as the OL-SRTs (p = 0.013, r = -0.64). For the minimum, the VM separation index of electrodes 7-4 and 7-8 were significantly correlated with the FN-SRTs (p = .042, r = -0.54 and p = .012, r = -0.64respectively). Most significant correlations were observed for the maximum. Here, the VM separation indices for 4-6 and 7-8 were correlated with the FN-SRTs (p = .031, r = -0.56 and p = .026, r = .026-0.58), while 4–6, 7–8 and 7–10 were correlated with the OL-SRTs (p =.034, r = -0.56; p = .021, r = -0.60 and p = .047, r = -0.53). Interestingly, the VM separation index of electrodes 7-8 showed significant correlations for all three evaluation options as well as containing the strongest correlation. The correlations for this electrode pair are also graphically shown in Fig. 9. All correlations found were negative, indicating that a larger VM separation index leads to a lower SRT, which for the OLSA means a better speech perception in noise.

#### 4. Discussion

#### 4.1. Similarity of SoE and VM data

Previous research already discovered a possible link between intraoperatively measured SoE and TIM/VM data (Franke-Trieger et al., 2022; Söderqvist et al., 2021). In both cited studies, no complete normalization of TIM/VM data or SoE was performed, instead graphical similarities were shown by using differently scaled axes for TIM/VM and SoE data. The main difference is how the probe electrode was incorporated into the normalization: Söderqvist et al. (2021) calculated an effective transimpedance Zeff by extrapolating a far-field component and near-field component, then used this Zeff for the comparison of TIM and SoE. Franke-Trieger et al. (2022) chose to ignore the value of the probe electrode and showed that the decay of the electric field in SoE and VM were similar. One study (Kopsch et al., 2022) also investigated the postoperative link between SoE and TIM, the comparison was however limited to the half-widths. Our normalization approach was closely aligned to the one used by Franke-Trieger et al. (2022) since we also focused on the far-field effect only and therefore ignored the probe electrode. To get a maximal similarity between the fitting of SoE and VM data, the probe electrode was assigned the normalized amplitude value of 0 in the min2-normalization approach. As this might affect the correlation between SoE and VM data, the probe electrode was not included in the correlation analysis.

Even so, a good alignment between the SoE and VM data could be found and adding to the findings of Söderqvist et al. (2021), we also found a correlation between postoperatively measured SoE and VM data in for most cases in our comparison dataset. However, the alignment was not perfect: differences between both measurements were visible, especially in the RMS-difference (see Figs. 5 and 6). The presence of some differences was expected, as the SoE contains more information than the VM. The VM mainly contains the geometric information of the spatial electric field spread, which is why it has been used to calculate insertion depth (Aebischer et al., 2021) or detect tip fold-overs (Beck et al., 2024; Hans et al., 2021; Klabbers et al., 2021). SoE on the other hand measures spatial masking of the electrodes through spreading electrical fields and is based on ECAPs, which also contain information about the neural interface as well as the spatial electrical field spread. The correlation analysis also showed the most significant correlations for the apical recording location and the least for the basal recording location, which is probably a result of the few data points available on the basal side of the basal recording location. This is especially the case for the CI-users, in which the most basal electrode (E12) is globally deactivated (S1r, S16l). Interestingly, this is in contrast to Kopsch et al. (2022), where the only significant correlation between SoE and TIM half-widths was found for the medial recording location. However, since P. Nachtigäller et al. Hearing Research 465 (2025) 109357



(caption on next column)

Fig. 7. Results of the parameters extracted from exponential fitting (box plots, outliers are denoted with crosses). A: widths at 25 % (DIST $_{0.25}$ ) and 50 % (DIST $_{0.5}$ ) relative peak amplitude for both SoE (white boxes) and VM (green boxes) data for the apical recording location (top), medial recording location (middle) and basal recording location (bottom). DIST $_a$  is the width to the apical side, DIST $_b$  the width to the basal side and DIST $_{ab}$  the sum DIST $_a$  + DIST $_b$ . B: measure of asymmetry  $\Delta$ Max $_a$  $_b$ , i.e., the difference of peak normalized amplitude of the apical and basal side for SoE (white boxes) and VM (green boxes) data.

the correlation was performed using the half-widths and not the recordings themselves, a comparison between the findings is difficult.

#### 4.2. Analysis of VM

When adapting the SoE-analysis of the previous paper (Rader et al., 2023) to the VM data, a similar pattern to the correlation analysis could be observed. The differences between SoE and VM data were again low for the apical recording location and largest for the basal recording location (see Fig. 7A), which was the case for both the boxplots and the statistical testing. While significant differences between the width measures of SoE and VM data were found, they were still quite similar. This is in agreement with the findings of Söderqvist et al. (2021) and Kopsch et al. (2022), who reported only weak or no correlations between 50 % widths of SoE and TIM. Further analysis by Söderqvist et al. (2021) showed, that a significant effect of recording location and an interaction between recording location and measurement type could be found. Kopsch et al. (2022) also only found a significant correlation for the medial recording location, adding to the effect of recording location. This was not specifically tested in our dataset, but the interaction is also visible in Fig. 7A: depending on the recording location, the significant differences in width parameters changed. A significant effect of measurement type was also reported by (Mohan et al., 2024). They reported variation between SoE and TIM widths as well and found more variability in the TIM widths compared to SoE widths, which was not the case for the dataset presented here. The measure of asymmetry  $\Delta Max_{ab}$ however was not found to significantly differ between VM and SoE data, which is an indication, that this asymmetry is likely a geometrical or anatomical feature, making the explanation of the tighter coils of the cochlear duct in the apex given in Abbas et al. (2004), Cohen et al. (2003) likely. The significant differences in the width measures were likely the reason, why the correlation with SRTs present in the SoE-analysis could not be replicated with the VM. Similarly, Kopsch et al. (2024) also found no significant correlation between width measures extracted from the TIM and monosyllabic word recognition. This together with the findings discussed in the previous section indicate, that SoE and VM do not contain the exact same information. While the VM contains information about the electric field distribution in the cochlea, the SoE measurement contains additional information: SoE also contains information about the neural interface and degree of masking between the electrodes, which is not present in the VM. Therefore, we conclude that SoE and VM can't always be used interchangeably. If the neural component is relevant, it is still necessary to use SoE, even though it has some disadvantages compared to the quicker and more easily measured VM. Still, the similarities of SoE and VM are considerable and for tasks that refer to electrode positioning like detecting tip fold-overs and estimating insertion depth, VM appears to be preferrable.

The ECAP separation index introduced by Hughes (2008) showed a promising correlation with pitch ranking, which in turn is related to speech perception. This metric was adopted to the VM data in this paper and evaluated. The values for the VM separation index were different from those published in Hughes (2008), which makes sense as the absolute sum used in the calculation does not compensate for the number of electrodes. The implants used in this study have 12 electrodes compared to the 22 used in Hughes (2008). If this is factored in, the data is more in agreement. The asymmetry found in the VM separation index

 $\begin{tabular}{ll} \textbf{Table 1}\\ \textbf{. List of CI-user implants, electrode arrays and etiologies. HL} = \textbf{hearing loss.}\\ \end{tabular}$ 

subject	CI left	Array left	CI right	Array right	etiology
S1	CONCERTO	FLEXsoft	CONCERTO	FLEX28	Progressive HL
S2	SONATAti100	Standard	SONATAti100	FLEXsoft	Progressive HL
S3	PULSARci100	Standard	CONCERTO	Standard	HL during infancy
S4	CONCERTO	FLEX28	CONCERTO	FLEX28	Congenital auditory defect
S5	PULSARci100	FLEX24	CONCERTO	FLEX28	HL during childhood
S6	PULSARci100	Medium	PULSARci100	Compressed	Meningitis
S7	CONCERTO	FLEX28	CONCERTO	FLEXsoft	Progressive HL
S8	C40+	Standard	PULSARci100	Standard	Progressive HL
S9	SONATAti100	Standard	SONATAti100	Standard	Progressive HL
S10	C40+	Standard	CONCERTO	FLEXsoft	Meningitis
S11	CONCERTO	FLEXsoft	CONCERTO	FLEXsoft	Progressive HL
S12	CONCERTO	FLEX28	PULSARci100	Standard	Progressive HL
S13	CONCERTO	FLEXsoft	C40+	Standard	Congenital deafness
S14	PULSARci100	Standard	PULSARci100	Standard	HL during childhood
S15	C40+	Standard	SONATAti100	Standard	Congenital auditory defect
S16	CONCERTO	FLEX28	CONCERTO	FLEX28	Progressive HL
S17	CONCERTO	FLEX28	CONCERTO	FLEX28	Congenital auditory defect

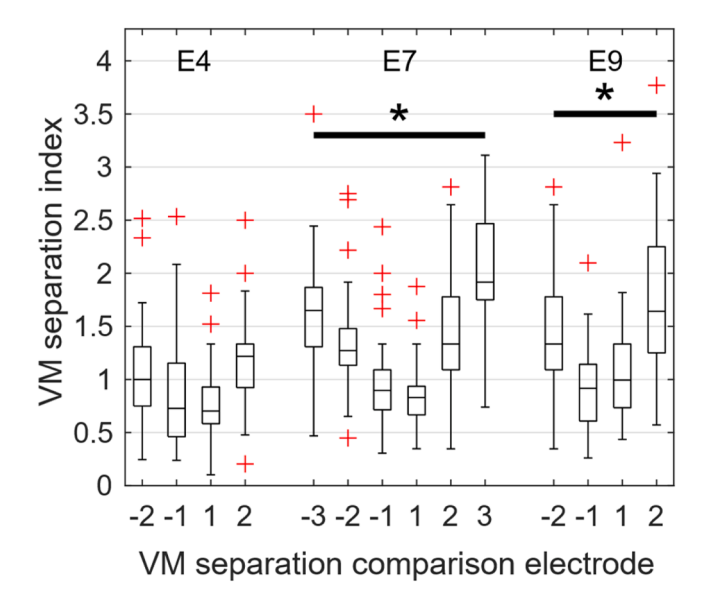


**Fig. 8.** Results of the VM separation index (box plots, outliers are denoted with crosses). The electrodes used for the calculation are shown at the top of the figure (E4, E7 and E9) and the relative distance to the comparation electrode is shown on the y-axis.

matches data published on the asymmetry in SoE- and VM-based width data discussed before, again indicating an anatomical or structural origin. In this study, we found significant correlations between the VM separation index and SRTs measured in a multi-source noise field. All correlations found were negative, meaning that a higher separation between the electrodes leads to a lower OLSA-SRT, which indicates a better listening performance in noise. This agrees with the hypothesis that a higher separation index, meaning less overlap of electrical spread patterns, is beneficial for the CI-user formulated in Hughes (2008), which we also applied here. The largest correlation was found for the VM separation index between electrodes 7 and 8, which in the used implants in most cases corresponds to center frequencies of 1.6 and 2.2 kHz respectively. These are also the electrodes where in most CI-users the charge applied through the mapping was highest. A probable explanation for this is that because of this comparably high charge for electrodes 7 and 8, the CI-users benefit from a higher VM separation index in this range as it provides them with additional cues through less overlap of the electrical field spread. Also, Fastl Noise has its masking peak at slightly higher frequencies (Fastl and Zwicker, 2007) while Oldenburg Noise has its masking peak at lower frequencies (Rader et al.,

2013). The frequencies of electrodes 7 and 8 still contribute to speech recognition but lie outside of the masking maximum of both noise conditions, which might affect the relationship between VM separation index and SRTs.

Additionally, the analysis method of Joly et al. (2021) was implemented and applied to our dataset. Joly et al. (2021) proposed a methodology of transforming the VM to a set of voltage curves, which are then fitted to a single exponential function, from which the exponent is extracted and labelled exponential spread coefficient (ESC). The values we calculated from our dataset were comparable to those published in Joly et al. (2021). For the inclusion of all patients, we found no correlation between the ESC and the SRT, which was also the case in Joly et al. (2021). However, they found a significant correlation if all CI-users with deactivated electrodes were excluded. For our dataset this was not feasible, as only 4 CI-users had the full array active for both ears. From our results we can't conclude whether this ESC is a good descriptor of the VM.

# 4.3. Limitations

This study has a number of limitations. The number of included CIusers is rather low, which is aggravated by the low number of analyzable SoE profiles for each recording location, resulting in fewer datapoints than desired. Additionally, many CI-users have deactivated electrodes, which might have influenced the findings of this paper. The probably largest limitation is the speech perception, which has only been measured in the bilateral best aided condition. Therefore, no analysis on peripheral effects could be conducted and the measures for each ear had to be combined, which is why different measures of combination were investigated, since both ears differ in extracted metrics. Another limitation concerns the correlations performed. Since a large number of correlations was calculated in this study, we chose not to adjust the significance level due to the multiple comparisons. This affects the significance of our reported correlations. However, since for correlations the correlation coefficient has more weight than the significance, we chose to focus on the correlation coefficients instead. Finally, this study has all the limitations inherent to a monocentric prospective study.

# 5. Conclusion

Previously shown similarities between SoE and VM data could be confirmed for postoperative measurements in patients fitted with long electrode arrays through a good visual match and significant correlations. Still, some differences in the measurements could be observed. Especially when evaluating the widths, significant differences between

P. Nachtigäller et al. Hearing Research 465 (2025) 109357

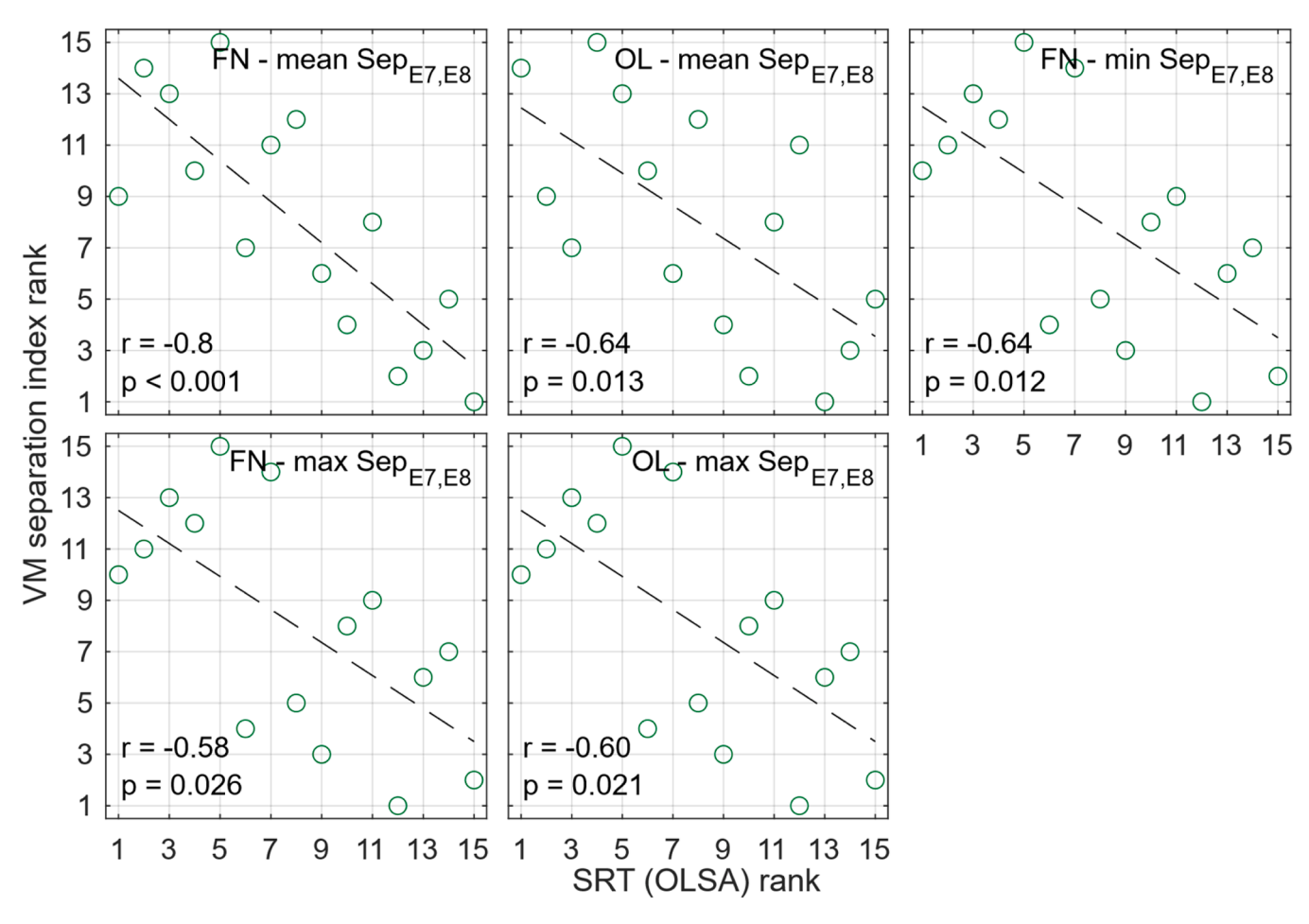


**Fig. 9.** Spearman correlations between ranked VM separation index results and ranked speech reception thresholds obtained either in Fastl (modulated) noise (FN) or continuous Oldenburg noise (OL) condition. Rank denotes the ordered values of VM separation index and SRT according to the spearman correlation coefficient. Presented are only the correlations for the VM separation index between the stimulating electrodes 7 and 8, which resulted in the largest correlations. Inset bottom left: Spearman rank correlation coefficients for SRT rank versus VM separation index rank. Inset top right: the exact parameters used for the correlation. FN = SRT with FASTL noise, OL: SRT with OLSA noise, Mean Sep<sub>E7,E8</sub>, Min Sep<sub>E7,E8</sub>, Max Sep<sub>E7,E8</sub>: Mean, Min and Max of the VM separation index between electrodes E7 and E8.

SoE and VM data were present. This leads us to the conclusion that SoE and VM show similarities through measuring the electrical field distribution, however the neural aspect included in the SoE measurement contains enough additional information that they can't be used completely interchangeably.

The novel adaptation of the ECAP separation index to the VM as the VM separation index showed promise through its correlation with the SRTs, but further research on this topic is necessary, especially its relation to the original ECAP separation index proposed by Hughes (2008). Also, the peripheral effect of the SoE and VM-based analysis methods on SRTs was not included in this study and needs further research.

# Compliance with ethical guidelines

All human studies described in this manuscript were performed in accordance with the national law and with the Declaration of Helsinki of 1975 (in its current revised version). The study was approved by the local ethical review board (University of Frankfurt, 228/14).

Data availability: Data will be made available on personal request to the corresponding author.

# CRediT authorship contribution statement

Pascal Nachtigäller: Validation, Methodology, Formal analysis,

Writing – original draft, Software, Investigation, Data curation, Writing – review & editing, Visualization. **Tobias Weissgerber:** Writing – original draft, Resources, Project administration, Writing – review & editing, Validation. **Uwe Baumann:** Writing – original draft, Resources, Writing – review & editing, Validation, Project administration. **Tobias Rader:** Writing – original draft, Validation, Resources, Methodology, Formal analysis, Conceptualization, Writing – review & editing, Visualization, Supervision, Project administration, Investigation, Data curation.

# **Declaration of competing interest**

There are no competing interests.

## Acknowledgements

We thank Stefan Strahl for his inspiration and helpful comments throughout the early stages of the manuscript. We also thank the participants in this study for their participation.

# Data availability

Data will be made available on request.

#### References

- Abbas, P.J., Brown, C.J., Shallop, J.K., Firszt, J.B., Hughes, M.L., Hong, S.H., Staller, S.J., 1999. Summary of results using the nucleus CI24M implant to record the electrically evoked compound action potential. Ear Hear 20 (1), 45–59. https://doi.org/10.1097/00003446-199902000-00005.
- Abbas, P.J., Hughes, M.L., Brown, C.J., Miller, C.A., South, H., 2004. Channel interaction in cochlear implant users evaluated using the electrically evoked compound action potential. Audiol. Neurootol. 9 (4), 203–213. https://doi.org/10.1159/000078390.
- Aebischer, P., Meyer, S., Caversaccio, M., Wimmer, W., 2021. Intraoperative impedance-based estimation of Cochlear implant electrode array insertion depth. IEEE Trans Biomed Eng. 68 (2), 545–555. https://doi.org/10.1109/TBME.2020.3006934.
- Beck, R., Aschendorff, A., Arndt, S., et al., 2024. Evaluation of insertion quality of a slim perimodiolar electrode array. Eur. Arch. Otorhinolaryngol 281, 1215–1220. https://doi.org/10.1007/s00405-023-08212-5.
- Cohen, L.T., Richardson, L.M., Saunders, E., Cowan, R.S., 2003. Spatial spread of neural excitation in cochlear implant recipients: comparison of improved ECAP method and psychophysical forward masking. Hear. Res. 179 (1–2), 72–87. https://doi.org/10.1016/S0378-5955(03)00096-0.
- Fastl, H., Zwicker, E., Springer series in Information sciences, 2007. Psychoacoustics: Facts and Models, (3rd ed.), 22. Springer, Berlin Heidelberg, pp. 353–356. https://doi.org/10.1007/978-3-540-68888-4. Imprint: Springer.
- Fetterman, B.L., Domico, E.H., 2002. Speech recognition in background noise of cochlear implant patients. Otolaryngol. Head Neck Surg. 126 (3), 257–263. https://doi.org/ 10.1067/mln.2002.123044.
- Franke-Trieger, A., Strahl, S., Janosch, A., Neudert, M., Zahnert, T., 2022. Intraoperative lagekontrolle von MEDEL elektroden mittels spread of excitation und spannungsmatrix. Jahrestagung der Deutschen Gesellschaft für Audiologie 24. https://doi.org/10.3205/22DGA175. Advance online publication(German Medical Science GMS Publishing House).
- Grolman, W., Maat, A., Verdam, F., Simis, Y., Carelsen, B., Freling, N., Tange, R.A., 2009. Spread of excitation measurements for the detection of electrode array foldovers: a prospective study comparing 3-dimensional rotational x-ray and intraoperative spread of excitation measurements. Otol. Neurotol. 30 (1), 27–33. https://doi.org/ 10.1097/mao.0b013e3181857ab.
- Hans, S., Arweiler-Harbeck, D., Kaster, F., Ludwig, J., Hagedorn, E., Lang, S., Meyer, M., Holtmann, L.C., 2021. Transimpedance matrix measurements reliably detect electrode tip fold-over in Cochlear implantation. Otol. Neurotol. 42 (10), e1494–e1502. https://doi.org/10.1097/MAO.0000000000003334.
- Hughes, M.L, 2008. A re-evaluation of the relation between physiological channel interaction and electrode pitch ranking in cochlear implants. J. Acoust. Soc. Am. 124 (5), 2711–2714. https://doi.org/10.1121/1.2990710.
- Joly, C.-A., Reynard, P., Hermann, R., Seldran, F., Gallego, S., Idriss, S., Thai-Van, H., 2021. Intra-cochlear current spread correlates with speech perception in experienced adult Cochlear implant users. J. Clin. Med. 10 (24), 5819. https://doi.org/10.3390/ jcm10245819.
- Klabbers, T.M., Huinck, W.J., Heutink, F., Verbist, B.M., Mylanus, E.A.M., 2021. Transimpedance matrix (TIM) measurement for the detection of intraoperative

- electrode tip foldover using the slim modiolar electrode: a proof of concept study. Otol. Neurotol. 42 (2), e124–e129. https://doi.org/10.1097/
- Klop, W.M.C., Hartlooper, A., Briare, J.J., Frijns, J.H.M, 2004. A new method for dealing with the stimulus artefact in electrically evoked compound action potential measurements. Acta Otolaryngol. 124 (2), 137–143. https://doi.org/10.1080/ 00016490310016901
- Kopsch, A.C., Rahne, T., Plontke, S.K., Wagner, L., 2022. Influence of the spread of electric field on neural excitation in cochlear implant users: transimpedance and spread of excitation measurements. Hear. Res. 424, 108591. https://doi.org/ 10.1016/j.heares.2022.108591. S.
- Kopsch, A.C., Rahne, T., Plontke, S.K., Wagner, L., 2024. Influence of the spread of the electric field on speech recognition in Cochlear implant users. Otol. Neurotol. 45 (3), e221–e227.
- Miller, C.A., Brown, C.J, Abbas, P.J, Chi, S.-L, 2008. The clinical application of potentials evoked from the peripheral auditory system. Hear. Res. 242 (1–2), 184–197. https://doi.org/10.1016/j.heares.2008.04.005.
- Mohan, P., Sinkkonen, S.T., Sivonen, V., 2024. The association of intraoperative electric field and neural excitation patterns of the cochlear implant with patient-related factors of age, gender, cochlear diameter, and postoperative speech measures. Hear. Res. 453, 109131. https://doi.org/10.1016/j.heares.2024.109131.
- Rader, T., Fastl, H., Baumann, U., 2013. Speech perception with combined electric-acoustic stimulation and bilateral cochlear implants in a multisource noise field. Ear Hear 34 (3), 324–332. https://doi.org/10.1097/AUD.0b013e318272f189.
- Rader, T., Nachtigäller, P., Linke, T., Weißgerber, T., Baumann, U., 2023. Exponential fitting of spread of excitation response measurements in cochlear implants.
  J. Neurosci. Methods 391, 109854. https://doi.org/10.1016/j.ineumeth.2023.109854.
- Söderqvist, S., Lamminmäki, S., Aarnisalo, A., Hirvonen, T., Sinkkonen, S.T., Sivonen, V., 2021. Intraoperative transimpedance and spread of excitation profile correlations with a lateral-wall cochlear implant electrode array. Hear. Res. 405, 108235. https://doi.org/10.1016/j.heares.2021.108235.
- The MathWorks Inc, 2024. MATLAB version: 24.2.0.2740171 (R2024b). The MathWorks Inc, Natick, Massachusetts. https://www.mathworks.com.
- Vozzi, A., Ronca, V., Malerba, P., Ghiselli, S., Murri, A., Pizzol, E., Babiloni, F., Cuda, D., 2022. An innovative method for trans-impedance matrix interpretation in hearing pathologies discrimination. Med. Eng. Phys. 102, 103771. https://doi.org/10.1016/ i.medengnby.2022.103771.
- Wagner, L., Plontke, S.K., Fröhlich, L., Rahne, T., 2020. Reduced spread of electric field after surgical removal of intracochlear schwannoma and cochlear implantation. Otol. Neurotol. 41 (10), e1297–e1303. https://doi.org/10.1097/ MA0.0000000000002884.
- Wagner, L., Plontke, S.K., Rahne, T., 2023. An analysis of the spread of electric field within the cochlea for different devices including custom-made electrodes for subtotal cochleoectomy. PloS One 18 (9), e0287216. https://doi.org/10.1371/ journal.pone.0287216.
- Zuniga, M.G., Rivas, A., Hedley-Williams, A., Gifford, R.H., Dwyer, R., Dawant, B.M., Sunderhaus, L.W., Hovis, K.L., Wanna, G.B., Noble, J.H., Labadie, R.F., 2017. Tip fold-over in Cochlear implantation: case series. Otol. Neurotol. 38 (2), 199–206. https://doi.org/10.1097/MAO.000000000001283.